# Determination of internuclear potentials from heavy-ion fusion excitation functions*

J. R. Birkelund and J. R. Huizenga
*Departments of Chemistry and Physics and Nuclear Structure Research Laboratory,† University of Rochester, Rochester, New York 14627*
(Received 20 July 1977)

The internuclear potential determined from published fusion barrier parameters is compared with the proximity potential of Blocki *et al.* Discussion is given of the uncertainties introduced into the data analysis by the effects of friction and errors in the barrier radii.

[NUCLEAR REACTIONS Fusion, determination of internuclear potentials from heavy-ion fusion excitation functions.]

In a recent paper[1] Scobel *et al.* have deduced fusion barrier parameters from a considerable number of well determined complete fusion excitation functions measured for $^{35}$Cl induced reactions on a series of targets with masses between $^{27}$Al and $^{124}$Sn. In principle the barrier parameters determined from complete fusion reactions may lead to a measurement of the internuclear potential at radial separations smaller than the separation region tested by elastic scattering measurements. However, because of the depth of interpenetration of the target and projectile necessary to reach the fusion barrier, the effect of nuclear friction cannot be ignored if the nuclear potential is to be extracted from fusion barrier parameters. In addition, since the nuclear potential is determined from the difference between the barrier height and the Coulomb potential, the deduced nuclear potential is very seriously affected by errors in the radial position of the barrier.

If friction is neglected in the analysis of fusion excitation functions, the fusion cross section $\sigma_f(E)$ at incident projectile energy $E$ is given by[1]

$$\sigma_f(E) = \pi R_B^2 (1 - V_B/E), \tag{1}$$

where $R_B$ is the $s$-wave barrier radius and $V_B$ is the barrier height obtained from the combination of the Coulomb potential $V_C$ and nuclear potential $V_N$:

$$V_N(R_B) = V_B(R_B) - V_C(R_B). \tag{2}$$

Barrier parameters are obtained from the data by fitting a straight line through a plot of $\sigma_f$ vs $1/E$. The slope and intercept of this line with the $1/E$ axis lead to the $s$-wave barrier radius and height, respectively. The *validity* of this analysis *requires* that *all* $l$ waves *contributing* to the *fusion cross section have the same barrier radius* $R_B$, a condition which is probably *not* fulfilled for most reactions.

If radial friction is dominant and included in the derivation of $\sigma_f(E)$ for the case of constant orbital angular momentum, Eq. (1) is modified to first order to

$$\sigma_f(E) = \pi R_B^2 \left(1 - \frac{V_B + E_F}{E}\right), \tag{3}$$

where $E_F$ is the energy loss due to radial friction on that portion of the trajectory in the entrance channel leading up to the barrier. The magnitude of the energy loss due to friction depends on the radial dependence of the friction forces near the barrier. For some systems it may be that the $s$-wave barrier lies close to or outside the range of the friction where $E_F$ is zero, and the friction correction included in Eq. (3) may be neglected. However, in most cases as the projectile energy increases, the $l$-dependent barriers move to smaller radii. Hence, the friction loss is expected to become more important than at the $s$-wave barrier radius and, in general, $E_f$ will be a function of the projectile energy. Qualitatively, the effects of radial friction on the derived nuclear potential may be seen by the assumption that $E_f$ is constant for the bombarding energies used in the data analysis. If $R_B$ is assumed constant also, then Eq. (3) represents a straight line with a $1/E$ axis intercept which leads to a value of $V_B + E_f$, and a slope related to the $s$-wave barrier radius by

$$\frac{d\sigma_f}{d(1/E)} = -\pi R_B^2 (V_B + E_F). \tag{4}$$

Thus, the effect of a neglect of radial friction in the analysis of fusion cross section data is to produce a value for the barrier which is too high and, hence, an underestimate of the absolute magnitude of the nuclear potential, if the barrier radius is independent of $l$. Tangential friction effects on measured fusion barriers are more difficult to estimate since tangential friction reduces both the kinetic energy and the orbital angular momen-

tum of the system. Preliminary classical trajectory calculations suggest that these two effects tend to compensate each other for projectile energies near the $s$-wave barrier and lead to only a small change in $\sigma_f$ at near-barrier energies. However, tangential friction markedly alters $\sigma_f$ at higher energies.

Further, in most cases the slope of the $\sigma_f$ vs $1/E$ curve is less well determined than the intercept on the $1/E$ axis, and this leads to an uncertainty in the barrier radius $R_B$. This uncertainty is further increased by the general dependence of the barrier distance on $l$, and hence projectile energy, which causes the $\sigma_f(E)$ vs $1/E$ curve to deviate from a linear function. An error in the barrier radius is reflected as error in the nuclear potential through Eq. (2), since an accurate knowledge of the radius is necessary to evaluate the large and strongly radial dependent Coulomb potential.

Scobel *et al.*[1] have compared the nuclear potential derived from their fusion data with various theoretical potentials. In Fig. 1 this comparison is extended, using the proximity potential of Blocki *et al.*[2] and nuclear potentials derived from fusion excitation functions listed in Table I. The fusion data for Fig. 1 were analyzed neglecting nuclear friction by the use of Eq. (1). The proximity potential is expressed as a function of the surface separation $\zeta$ and given by[2]

$$V_N(\zeta) = 4\pi\gamma [C_T C_P/(C_T + C_P)] b\Phi(\zeta), \tag{5}$$

where

$$\gamma = 0.9517\{1 - 1.7826[(N_T + N_P - Z_T - Z_P)/(A_T + A_P)]^2\},$$

$$C_i = R_i[1 - (b/R_i)^2 + \cdots],$$

$$R_i = 1.28A_i^{1/3} - 0.76 + 0.8A_i^{-1/3},$$

$$\zeta = r - C_T - C_P,$$

$$b = 1 \text{ fm}.$$

The quantity $\Phi(\zeta)$ is a universal function given by Blocki *et al.*[2] Thus an experimental value for $\Phi(\zeta_B)$ at the fusion barrier is given by

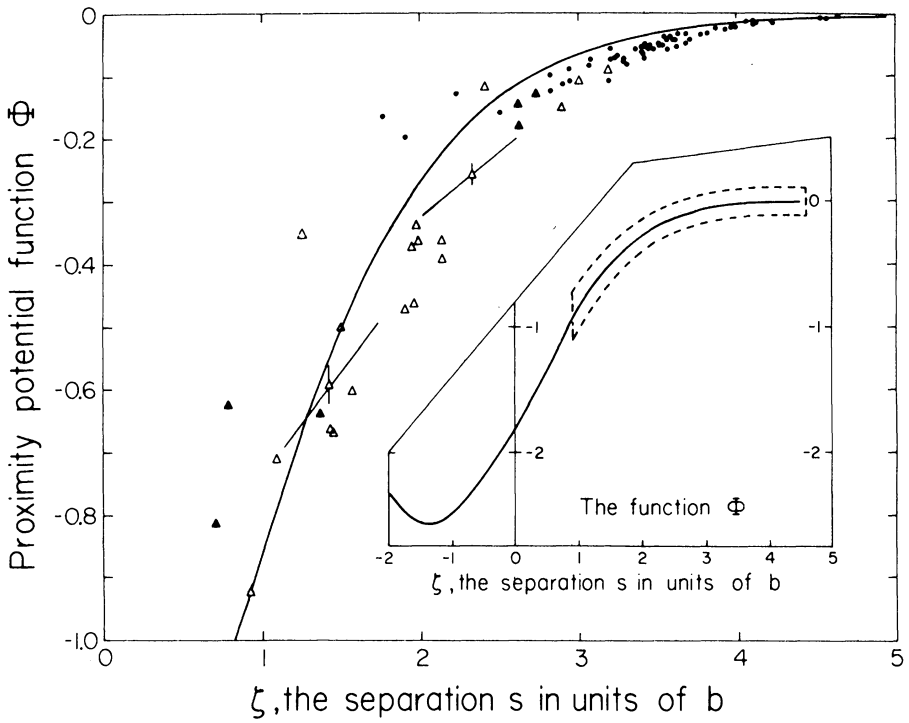


FIG. 1. A comparison of the universal proximity potential (Ref. 2) $\Phi(\zeta)$ as a function of the dimensionless quantity $\zeta$ (solid line) with experimental data (points). The analysis of elastic scattering data (Ref. 3) produces the circles and the analysis of inelastic reaction data produces the triangles. The open triangles are based on excitation function measurements of fusion cross sections by counter-telescope measurements of evaporation residuals and/or fission fragments, while the filled triangles rely on excitation functions based on summing measured partial fusion cross sections. The latter values are subject to the largest errors. The region enclosed by the dashed line in the insert shows the part of the proximity potential tested by experimental data. Errors in $\zeta$ are reflected also in $\Phi$ (see text) as illustrated for two fusion points.

TABLE I. Barrier parameters measured from experimental fusion excitation functions by use of Eq. (1).

| Reaction | $R_B$ (exp.) (fm) | $V_B(R_B)$ (exp.) (MeV) | $-V_N(R_B)$ (exp.) (MeV) | $C_P$ (fm) | $C_T$ (fm) | $\gamma$ (MeV fm$^{-2}$) | $\frac{4\pi\gamma C_T C_P}{C_T+C_P}$ (MeV fm$^{-1}$) | $\zeta_B$ (exp.) (fm) | $-\Phi(\zeta_B)$ (exp.) | $R_B$ theory (fm) | Ref. |
|---|---|---|---|---|---|---|---|---|---|---|---|
| $^{4}$He+$^{152}$Dy | 9.9±0.2 | 17.1±0.1 | 2.1±0.1 | 1.21 | 6.06 | 0.9238 | 11.704 | 2.63±0.2 | 0.179±0.008 | 9.74 | 10 |
| $^{4}$He+$^{233}$U | 9.8±0.6 | 24.0±0.2 | 5.6±0.2 | 1.21 | 7.11 | 0.8791 | 11.420 | 1.51±0.6 | 0.495±0.02 | 10.66 | 14 |
| $^{7}$Li+$^{159}$Tb | 8.6±0.2 | 23.7±0.1 | 9.0±0.1 | 1.63 | 6.16 | 0.8963 | 14.518 | 0.79±0.2 | 0.622±0.007 | 10.20 | 10 |
| $^{12}$C+$^{12}$C | 6.65 | 6.17 | 1.63 | 2.12 | 2.12 | 0.9517 | 13.996 | 2.41 | 0.116 | 7.32 | 11 |
| $^{12}$C+$^{152}$Sm | 10.9±0.3 | 46.8±0.2 | 2.3±0.2 | 2.12 | 6.06 | 0.9022 | 17.806 | 2.73±0.3 | 0.129±0.02 | 10.27 | 10 |
| $^{16}$O+$^{12}$C | 7.55 | 7.69 | 1.46 | 2.42 | 2.12 | 0.9517 | 13.515 | 3.01 | 0.108 | 7.49 | 11 |
| $^{16}$O+$^{27}$Al | 8.1±0.15 | 16.1±0.6 | 2.4±0.6 | 2.42 | 3.05 | 0.9508 | 16.135 | 2.63±0.15 | 0.148±0.04 | 8.07 | 15 |
| $^{16}$O+$^{148}$Nd | 9.8±0.2 | 57.8±0.5 | 12.8±0.5 | 2.42 | 6.00 | 0.9240 | 20.023 | 1.37±0.2 | 0.64 ±0.03 | 10.41 | 10 |
| $^{16}$O+$^{208}$Pb | 11.4±0.8 | 74.8±2 | 8.2±2 | 2.42 | 6.82 | 0.8830 | 22.446 | 2.14±0.8 | 0.36 ±0.09 | 11.10 | 12 |
| $^{18}$O+$^{12}$C | 9.3±0.2 | 7.51 | 1.28 | 2.55 | 2.12 | 0.9442 | 13.735 | 3.19 | 0.093 | 7.66 | 11 |
| $^{18}$O+$^{148}$Nd | 7.86 | 58.3±0.8 | 16.3±0.8 | 2.55 | 6.00 | 0.8963 | 20.155 | 0.71±0.2 | 0.81 ±0.04 | 10.59 | 10 |
| $^{19}$F+$^{12}$C | 7.64 | 8.08 | 2.1 | 2.62 | 2.12 | 0.9499 | 13.988 | 2.90 | 0.150 | 7.65 | 11 |
| $^{32}$S+$^{24}$Mg | 8.5±0.3 | 27.8±0.3 | 4.7±0.3 | 3.27 | 2.90 | 0.9495 | 18.339 | 2.3 ±0.3 | 0.26 ±0.02 | 8.49 | 9 |
| $^{32}$S+$^{27}$Al | 8.3±0.3 | 29.2±0.2 | 6.9±0.2 | 3.27 | 3.05 | 0.9512 | 18.863 | 1.98±0.3 | 0.37 ±0.01 | 8.62 | 9 |
| $^{32}$S+$^{40}$Ca | 9.0±0.3 | 43.2±0.2 | 8.0±0.2 | 3.27 | 3.59 | 0.9504 | 20.438 | 2.14±0.3 | 0.39 ±0.01 | 8.96 | 9 |
| $^{35}$Cl+$^{27}$Al | 8.4±0.2 | 30.7±0.4 | 7.2±0.4 | 3.40 | 3.05 | 0.9499 | 19.191 | 1.95±0.2 | 0.38 ±0.02 | 8.73 | 1 |
| $^{35}$Cl+$^{48}$Ti | 8.7±0.3 | 49.2±0.6 | 12.7±0.6 | 3.40 | 3.87 | 0.9455 | 21.504 | 1.43±0.3 | 0.59 ±0.03 | 9.35 | 1 |
| $^{35}$Cl+$^{56}$Fe | 9.5±0.4 | 59.5±1 | 7.5±1.0 | 3.40 | 4.12 | 0.9466 | 22.158 | 2.0 ±0.4 | 0.34 ±0.05 | 9.52 | 1 |
| $^{35}$Cl+$^{58}$Ni | 9.0±0.2 | 61.3±0.3 | 14.9±0.3 | 3.40 | 4.17 | 0.9499 | 22.357 | 1.43±0.2 | 0.67 ± 0.01 | 9.53 | 1 |
| $^{35}$Cl+$^{60}$Ni | 9.2±0.2 | 61.0±0.3 | 13.5±0.3 | 3.40 | 4.23 | 0.9470 | 22.431 | 1.57±0.2 | 0.60 ±0.01 | 9.60 | 1 |
| $^{35}$Cl+$^{62}$Ni | 9.6±0.2 | 60.8±0.3 | 10.6±0.3 | 3.40 | 4.29 | 0.9429 | 22.472 | 1.91±0.2 | 0.47 ±0.01 | 9.67 | 1 |
| $^{35}$Cl+$^{64}$Ni | 9.7±0.2 | 60.3±0.3 | 10.4±0.3 | 3.40 | 4.34 | 0.9377 | 22.564 | 1.96±0.2 | 0.46 ±0.01 | 9.73 | 1 |
| $^{35}$Cl+$^{90}$Zr | 9.8±0.2 | 84.0±0.5 | 15.9±0.5 | 3.40 | 4.96 | 0.9386 | 23.793 | 1.44±0.3 | 0.67 ±0.01 | 10.20 | 1 |
| $^{35}$Cl+$^{116}$Sn | 9.8±0.4 | 102.3±0.9 | 22.6±0.9 | 3.40 | 5.47 | 0.9302 | 24.509 | 0.93±0.4 | 0.92 ±0.04 | 10.62 | 1 |
| $^{35}$Cl+$^{124}$Sn | 10.1±0.4 | 104.0±0.8 | 17.2±0.8 | 3.40 | 5.61 | 0.9098 | 24.203 | 1.09±0.4 | 0.71 ±0.03 | 10.77 | 1 |
| $^{40}$Ar+$^{109}$Ag | 10.2[a] | 110.6[a] | 8.8 | 3.59 | 5.34 | 0.9241 | 24.929 | 1.27 | 0.35 | 10.72 | 13 |

[a]These values of $R_B$ and $V_B(R_B)$ are obtained from the two lowest energy data points (Ref. 13). With the reported errors in these two points, the values of $[R_B, V_B(R_B)]$ range from (13.0 fm, 115 MeV) to (8.9 fm, 94 MeV). The equivalent values of $[\zeta_B, -\Phi(\zeta_B)]$ are (4.0 fm, −0.86) and (−0.04 fm, 1.71), respectively. Although the first limit is meaningless, the wide range of allowed values of $\zeta_B$ and $\Phi(\zeta_B)$ for this reaction illustrate the importance of precise data in fixing $R_B$ before a meaningful comparison can be made between the experimental and theoretical nuclear potential.

$$\Phi_{\exp}(\zeta_B) = V_N(R_B)\{4\pi\gamma[C_T C_P/(C_T+C_P)]b\}^{-1}, \quad (6)$$

where

$$\zeta_B = R_B - C_T - C_P .$$

The experimental values of $\Phi(\zeta_B)$ are compared with the theoretical curve in Fig. 1. The triangles represent values obtained from fusion data, and the full dots indicate values obtained from elastic scattering using the method of Christensen and Winther.[3] In addition, the open triangles in Fig. 1 are based on excitation function measurements of fusion cross sections by counter telescope measurements of evaporation residues and/or fission fragments, while the filled triangles rely on excitation functions based on summing measured partial fusion cross sections. The latter values are subject to the largest errors. Figure 1 shows the smaller surface separation region tested by the fusion data. There is a qualitative agreement between the data and the theoretical proximity potential down to surface separations of 1 fm. However, the experimental potentials are systematically deeper than the proximity potential.

The errors shown in Table I arise from the uncertainty in the slope of the $\sigma_f$ vs $1/E$ line which causes an error in $R_B$, and in the intercept on the $1/E$ axis which causes an error in $V_N(R_B)$ and, hence, in $\Phi(\zeta_B)$. Thus the error in $V_N(R_B)$ produced by an error in $R_B$ is not included in Table I. Errors in the barrier radius alter both $\zeta(R_B)$ and $V_N(R_B)$ through the Coulomb potential in Eq. (2) and cause the fusion data points in Fig. 1 to move roughly parallel to the theoretical curve as shown by the slanted error bars in Fig. 1. Thus the agreement between the proximity potential and the measured values of $V_N$ from fusion is not altered greatly by errors in $R_B$. However, there remains considerable uncertainty concerning the actual magnitude of $V_N(R_B)$, because of uncertainty in $R_B$, even if a friction free analysis is accepted. The effect of including friction in the analysis is to increase the magnitude of the derived nuclear potential, thus moving the fusion data point below the theoretical curve in Fig. 1. However, there is at present no simple method for the estimation of the energy loss due to friction. Seglie, Sperber, and Sherman[4] have used the proximity nuclear potential together with friction described by a form factor of range to $\zeta = 4.0$ fm in a classical trajectory calculation of the critical angular momentum for fusion. These calculations give reasonable agreement with experimental critical angular momenta for some heavy-ion reactions. Randrup[5] in a proximity formulation of nuclear friction suggests that the range of the friction should be to $\zeta = 3.2$ fm. In both of these cases, the friction is effective before the projectile reaches the barrier, and cannot be ignored in analysis of fusion excitation functions.

The experimentally determined values of $R_B$ may be compared with the values expected from the proximity potential by use of an approximate expression for $\Phi(\zeta)$ given by Blocki *et al.*[2] For values of $\zeta > 1.2511$ the position of the barrier is given by

$$R_B \exp\left(-\frac{R_B}{1.5}\right) = K\left(\frac{Z_T Z_P (C_T+C_P)}{\gamma C_T C_P}\right)^{1/2} \exp\left(-\frac{C_T+C_P}{1.5}\right), \quad (7)$$

where $K$ is a universal constant. The experimental barrier radii are compared with the values derived from the proximity potential in Table I. As can be seen from the data in this table, the proximity potential, without including friction, gives qualitative agreement with the experimental radii.

A method for fusion excitation function analysis has been recently suggested by Bass[6] in which the nuclear potential is extracted at distances inside the $l = 0$ barrier by measurements of the slope of the $\sigma_f$ vs $1/E$ curve at energies where this function is no longer a straight line. In the Bass analysis the slope of a tangent drawn to the $\sigma_f$ vs $1/E$ curve gives the barrier position and the intercept of the tangent on the $1/E$ axis gives the barrier height. This method is greatly affected in accuracy by uncertainty in the barrier position since the slope of the tangent is not well determined by data currently available in the higher energy range. The Bass analysis leads to estimates of the nuclear potential which lie on curves roughly parallel to the theoretical proximity potential curve extending over a range of $\zeta$ values. However, with currently available data no precise value for the $\zeta$ value tested is obtained. Of more fundamental significance, Bass purports to sample $\zeta$ values smaller than the $s$-wave barrier where the effects of friction are even more important than for measurements of the $s$-wave barrier.

The effect of friction is also important for the analysis of fusion cross sections by use of the method suggested by Glas and Mosel[7,8] which depends upon the concept of a critical separation necessary for fusion. In the Glas and Mosel analysis the fusion excitation function near the $s$-wave barrier is given by Eq. (1), while at higher energies the asymptotic expression for the excitation function is given by

$$\sigma_f(E) = \pi R_{CR}^2 \left(1 - \frac{V_{CR}}{E}\right), \quad (8)$$

where $R_{CR}$ is the critical radius and $V_{CR}$ is the conservative potential at the critical radius ($R_{CR} < R_B$). In view of the important role of friction and energy dissipation at higher energies and smaller separation distances, the validity of Eq. (8) is questionable.

In summary, the analysis of fusion data for the nuclear potential at the barrier is complicated in principle by the difficulties involved in a calculation of the frictional energy loss, and in practice by the problem of measurement of excitation functions with sufficient accuracy to closely define the barrier radius. Until these two problems are adequately solved, it is not possible to make quantitative comparisons between the nuclear potential derived from fusion data and theoretical nuclear potentials. A more quantitative discussion of the importance of friction on fusion excitation functions will be reported elsewhere.

---

*Work supported by the U. S. Energy Research and Development Administration.

†Supported by a grant from the National Science Foundation.

[1]W. Scobel, H. H. Gutbrod, M. Blann, and A. Mignerey, Phys. Rev. C 14, 1808 (1976).

[2]J. Blocki, J. Randrup, W. J. Swiatecki, and C. F. Tsang, Ann. Phys. (N.Y.) 105, 427 (1977).

[3]P. R. Christensen and A. Winther, Phys. Lett. 65B, 19 (1976).

[4]E. Seglie, D. Sperber, and A. Sherman, Phys. Rev. C 11, 1227 (1975).

[5]J. Randrup, NORDITA report, December, 1976 (unpublished).

[6]R. Bass, Phys. Rev. Lett. 39, 265 (1977).

[7]D. Glas and U. Mosel, Nucl. Phys. A237, 429 (1975).

[8]U. Mosel, in Proceedings of the Symposium on Macroscopic Features of Heavy-Ion Collisions, Argonne [ANL/PHY-76-2, 1976 (unpublished)], Vol. 1, p. 341.

[9]H. H. Gutbrod, W. G. Winn, and M. Blann, Nucl. Phys. A213, 267 (1973).

[10]R. Broda, M. Ishihara, B. Herskind, H. Oeschler, and S. Ogaza, Nucl. Phys. A248, 356 (1975).

[11]P. Sperr, T. H. Braid, Y. Eisen, D. G. Kovar, F. W. Prosser, J. P. Schiffer, S. L. Tabor, and S. Vigdor, Phys. Rev. Lett. 37, 321 (1976).

[12]F. Videbaek, R. B. Goldstein, L. Grodzins, S. G. Steadman, T. A. Belote, and J. B. Garrett, Phys. Rev. C 15, 954 (1977).

[13]H. C. Britt, B. H. Erkilla, R. H. Stokes, H. H. Gutbrod, F. Plasil, R. L. Ferguson, and M. Blann, Phys. Rev. C 13, 1483 (1976).

[14]J. R. Huizenga, R. Vandenbosch, and H. Warhanek, Phys. Rev. 124, 1964 (1961).

[15]J. Dauk, K. P. Lieb, and A. M. Kleinfeld, Nucl. Phys. A241, 170 (1975).